Chemical Engineering Journal 158 (2010) 213–219

Contents lists available at ScienceDirect

Chemical Engineering Journal

journal homepage: www.elsevier.com/locate/cej

Adsorption of complex phenolic compounds on active charcoal: Breakthrough curves

Dominique Richard [a,*], Maria de Lourdes Delgado Núñez [a,b], Daniel Schweich [a]

[a] Université de Lyon, CNRS, Laboratoire de Génie des Procédés Catalytiques, CPE Lyon, 43 bd du 11 novembre 1918, BP 82077, 69616 Villeurbanne Cedex, France
[b] Universidad Autónoma Metropolitana, Av. San Pablo 180 col. Reynosa, 02200 México, Mexico

ARTICLE INFO

Article history:
Received 27 February 2009
Received in revised form
22 December 2009
Accepted 30 December 2009

Keywords:
Activated carbon
Adsorption
Catechol
Breakthrough curve
HSDM

ABSTRACT

The transient adsorption of catechol from aqueous solution ($C^0 = 5\,kg/m^3$) on activated carbon in an upflow fixed-bed column at 293 K was studied. The critical time at which the early breakthrough of the maximum admissible concentration ($C_{crit} = 0.3 \times 10^{-3}\,kg/m^3$) occurs is deduced from a Homogeneous Surface Diffusion Model (HSDM) that accounts for adsorption equilibrium and mass-transfer kinetics. The mass-transfer coefficient is measured using a thin bed adsorption method and a correlation is proposed to account for its dependence with the flow rate. The sensitivity of the model for the prediction of the critical time to the different parameters is discussed and it is found to be mostly dependant upon the mass-transfer coefficient K_f and the adsorbant mean particle diameter d_P. In addition, the critical time has been proved to increase with the adsorption capacity q_{max}. The existence of an optimal flow of polluted effluent through the column to achieve the removal of the pollutant with the highest efficiency is observed.

1. Introduction

Phenols constitute a widespread and important class of water pollutants and are considered as priority pollutants. Phenolic compounds are found amongst other places, in the waste waters of agro-industrial processes like the olive oil mills, tomato processing and wine distilleries [1,2].

A process has been proposed [3,4] to reduce the phenolic content of aqueous effluents, which involves the adsorption of the phenols on active charcoal before their catalytic hydrogenation. To properly design and operate fixed-bed adsorption processes, the adsorption isotherm and the fixed-bed dynamics, that is, the pollutant breakthrough curves, must be known. In a previous work [5], the adsorption equilibria of five phenolic compounds: tyrosol, catechol, veratric acid, vanillic acid and caffeic acid, on an activated carbon have been investigated.

A recent review [6] of adsorption of phenols on activated carbon has been dedicated to the thermodynamical aspects: effects of carbon surface functionalities, pH of solution, substituents of the phenolic compounds. However there is no mention of the kinetic aspects of the adsorption process (neither in a stirred tank nor in a column).

The present paper is devoted to the kinetic study of the adsorption of catechol, chosen as a model molecule, on a fixed-bed of active charcoal and to the modelling of the breakthrough curves. To predict the breakthrough curve with a sophisticated mass-transfer model, one needs many parameters that must be determined by independent kinetic study or estimated by suitable correlations. Dealing with a purification process it is not necessary to describe the full pattern of the breakthrough curve. Indeed only the start-up of this curve is of interest for such a process and the criteria which allow for evaluating the performance of the purification process are the residual pollutant outlet concentration that must be below a critical concentration, and the critical time that corresponds to the breakthrough of this critical concentration. Since while dealing with depollution by adsorption of pollutants, the critical concentration may be very low (and in any case below the authorized value), the study of the adsorption during the initial part of the breakthrough curve deserves a special attention.

Although the removal of phenolic compound from water effluents through adsorption on activated carbons [7,8] or other adsorbents like bark [9], activated sludges [10], resins [11,12] or modified alumina [13] has been the object of many studies in order to simulate or predict the pattern of the breakthrough curves, only few of them address the question of the critical time estimation which is a requirement in depollution processes where the aim is to release pollutant-free water.

* Corresponding author. Tel.: +33 4 72 43 17 52; fax: +33 4 72 43 16 73.
E-mail address: dri@lobivia.cpe.fr (D. Richard).

1385-8947/$ – see front matter © 2010 Elsevier B.V. All rights reserved.
doi:10.1016/j.cej.2009.12.044

Nomenclature

A	factor in the Yoshida correlation [32]
Bi	Biot number ($Bi = K_f \cdot d_P \cdot C^0/2 \cdot D_e \cdot \rho_p \cdot q_e$)
C_e	concentration of adsorbate in the liquid phase at equilibrium (kg/m^3)
$C_{b,i}$	concentration in the bulk in cell i of the model (kg/m^3)
C^0	inlet concentration of adsorbate solution (kg/m^3)
$C_{s,i}$	concentration at the surface in cell i of the model (kg/m^3)
D_e	effective diffusion coefficient (m^2/s)
D_m	molecular diffusion coefficient (m^2/s)
d_P	average particle diameter (m)
$h_{\min}$	minimal bed height (m)
k_L	Langmuir isotherm coefficient (m^3/kg)
K_f	film mass-transfer coefficient (m/s)
m	mass of adsorbant (active charcoal) in the adsorption column (kg)
μ	dynamic viscosity (Pa s)
N_{cell}	number of stirred tanks used in the model
q_e	uptake of substrate adsorbed at equilibrium (kg/kg$_{AC}$)
Q_l	flow rate (m^3/s)
$q_{\max}$	maximum uptake of substrate adsorbed on AC (kg/kg$_{AC}$)
Re	Reynolds number ($Re = \rho \cdot u_v \cdot d_P/\mu$)
S	specific surface area (m^2/g)
Sc	Schmidt number ($Sc = \mu/\rho \cdot D_m$)
Sh	Sherwood number ($Sh = K_f \cdot d_P/D_m$)
t_C	critical time (s)
u_v	superficial velocity (m/s)
V_{bed}	bed volume (m^3)
ϵ_B	bed porosity
ϵ_p	internal porosity of the active charcoal
ψ	shape factor in the Yoshida correlation [32]
ρ	fluid specific mass (kg/m^3)
ρ_p	particle specific mass (kg/m^3)
ρ_t	bed specific mass (kg/m^3)
[X]	concentration of species X (kg/m^3)

Subscripts

av.	average value
max	maximum value
s	surface value

Superscripts

0	initial value
*	dimensionless concentration ($C_x^* = C_x/C^0$)

2. Experimental

2.1. Materials

The phenolic compounds were purchased from Aldrich (L'Isle d'Abeau, France) and used as received. The activated charcoal Picactif TE80® was kindly provided by Pica (Vierzon, France). Its characteristics are reported in Table 1. Deionized water was used to prepare the solutions of the phenolic compounds. The phenol concentration was measured by UV spectrometry at its maximum of absorption ($\lambda = 225$ nm for catechol) using an UV–vis JASCO® UV-980 detector.

Table 1
Characteristics of Picactif TE80®.

Specific surface area	S	1370 m^2/g
Internal porosity	ϵ_p	0.563
Density of the particles	ρ_p	966 kg/m^3

2.2. Apparatus and measurement procedure

The fixed-bed adsorption experiments were carried out in a column 0.019 m i.d. and 0.25 m long which allows for a maximum amount of about 0.031 kg of active charcoal. The liquid flow rates used are within the 1×10^{-7}–1×10^{-6} m^3/s range (space velocity 0.0019–0.019 m/s).

The packing of the column with active carbon is carefully carried out in order to minimize band spreading and to prevent the presence of air bubbles. For the latter reason the active charcoal is previously outgased by stirring it in deionized water under ultrasonication for 5 min and the wet active charcoal is introduced stepwise into the column partially filled with water and after each addition, the column is tapped. When the column is filled and closed, deionized water is passed through and the background signal of the UV detector is recorded. A solution of the phenolic compound is then passed through the column and the absorbance of the outgoing solution is recorded to measure its concentration and hence the breakthrough curve.

The short bed adsorber (SBA) [14] experiments were carried out in a 0.014 m i.d. and 0.04 m high column with a solution of catechol of 5 kg/m^3 at flow rates in the 3.4×10^{-8}–3.1×10^{-7} m^3/s range.

3. Results and discussion

3.1. Fixed-bed adsorption

The performance of fixed-bed adsorption for a given flow of polluted effluent (flow rate Q_l and pollutant concentration C^0) are evaluated by the critical time and the amount of adsorbate fixed at that time. Fig. 1 shows these values for a critical concentration of 0.3×10^{-3} kg/m^3. For flow rate between 1×10^{-6} and 0.175×10^{-6} m^3/s and a feed solution at 5 kg/m^3, the amount of catechol adsorbed at the critical time does not depend upon the flow rate and is close to 65% of the maximum amount. At higher flow rate the amount of catechol adsorbed at the critical time decreases. Thus for this column, the optimal flow rate is close to 0.175×10^{-6} m^3/s.

3.2. Modelling of fixed-bed adsorption

A general approach to the description of the pollutant in the liquid phase close to the adsorbent grains making the fixed-

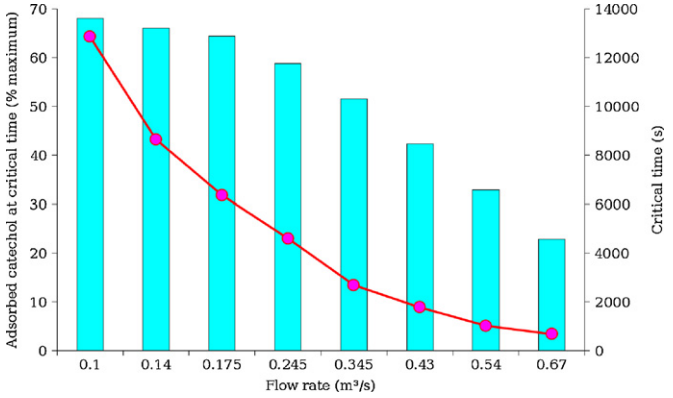

Fig. 1. Amount of adsorbed catechol (bars) and critical time (dots) as a function of the flow rate.

bed should consider four kinetic resistances to the mass transfer, i.e.:

(i) the external transport,
(ii) the diffusion within the liquid phase inside the grain,
(iii) the adsorption at the surface of the active carbon,
(iv) the surface diffusion.

Although rigorous this description is often oversophisticated because: (1) it involves too many parameters that need to be adjusted and (2) the effects of these processes on the shape of the breakthrough curve are almost identical and they cannot be determined independently from macroscopic experiments. Thus simplified models are required for application purposes. The simplest and most frequently used model for the external transport is the film model, introduced by Whitman [15]. Concerning the diffusion inside the grain, three classes of model have been proposed [16]:

- the Homogeneous Surface Diffusion Model (HSDM) [17,14] which considers that the sorbate is first adsorbed on the external surface of the grain and then diffuse inside the grain, the porous solid being seen as a pseudo-homogeneous medium,
- the Pore Diffusion Model (PDM) [18] considers that after going through the boundary layer, the substrate diffuses inside the liquid filling the pores and that adsorption only occurs on the internal surface of the grains,
- the Pore Surface Diffusion Model (PSDM) [19] considers that both phenomena occur simultaneously.

The HSDM which is widely referred to in the literature [20–26] and has led to the simulation of the fixed-bed adsorption of many organic compounds or ionic species on active charcoal or other adsorbents [27,28].

Thus, the HDSM model used in the present work relies on the following assumptions:

(1) One-dimensional plug-flow.
(2) The particles behave as a pseudo-homogeneous medium wherein the pollutant diffuses.
(3) External mass-transfer limitation is accounted for.
(4) Adsorption equilibrium prevails at the fluid–solid external surface.

As a consequence of the non-linearity of the adsorption isotherm, the set of equations resulting from the hypotheses is not solvable analytically and a numerical method has to be used. The details of the equation derivation are given in Appendix A.

3.3. Determination of the mass-transfer parameters

The quality of the model used to describe the fixed-bed adsorption of the phenolic pollutant considered, rely upon the validity of the thermodynamic and kinetic parameters involved. The isotherm adsorption parameters are reported in a previous paper [5]. The estimation of the effective diffusivity (D_e) and of the film mass-transfer coefficient (K_f) will be discussed now.

The effective diffusivity (D_e) has to be estimated from the kinetics of adsorption either in batch or fixed-bed reactor [29].

The mass-transfer coefficient (K_f) is often derived from semi-empirical correlations relating the Reynolds (Re), Schmidt (Sc) and Sherwood (Sh) numbers. Some of the correlations encountered for fixed-bed reactors are summarized in Table 2.

However the value of K_f estimated from the correlations may be false since they may have been established with packing conditions and nature of the grains different from those used in an other experimental study. An alternative approach [35] is to directly measure the value of K_f in a fixed-bed with similar characteristics.

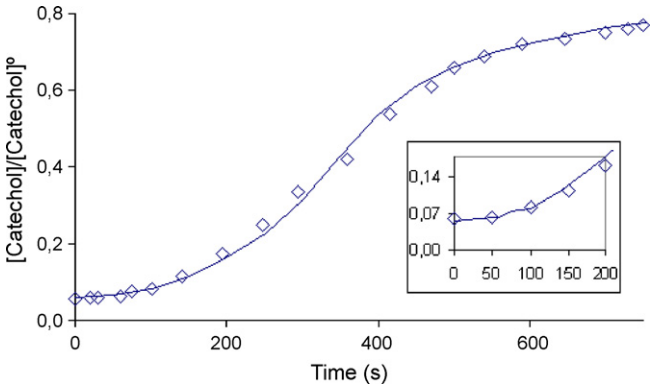

Fig. 2. Breakthrough curve experimental (◊) and calculated (line) of catechol through a micro-column (0.04 m height at 293 K with a flow rate of 0.14×10^{-6} m^3/s and a catechol concentration of 6 kg/m^3).

The method of Weber and Liu [35,36] was used which allows for the simultaneous determination of K_f and D_e from adsorption data collected with a column short enough for the initial outlet concentration to be different from zero. In this case it is possible to separate the effects of external transfer and internal diffusion in the grain since the initial step of adsorption is always controlled by the external transport. K_f is determined from the initial intercept of the breakthrough curve and then D_e is estimated via a regression along the breakthrough curve (cf. Fig. 2). In order to neglect the axial dispersion, the minimal bed height (h_{min}) must satisfy the condition:

$$\frac{h_{min}}{d_p} \geq 20$$

.

The average effective diffusivity determined for flow rates between 3.4×10^{-8} and 3.1×10^{-7} m^3/s for catechol is $D_e = 1.4 \times 10^{-11}$ m^2/s. The value of K_f depends upon the flow rate and the values measured are reported in Fig. 3. In this figure are also reported the value of K_f derived from some of the previously mentioned correlations. The measured values are close to those derived from the Wilson and Geankoplis correlation. Due to this similarity it is possible to derive a new correlation based upon the present measurements:

$$Sh = 1.38\epsilon^{-2/3} Re^{0.34} Sc^{1/3} \quad (1)$$

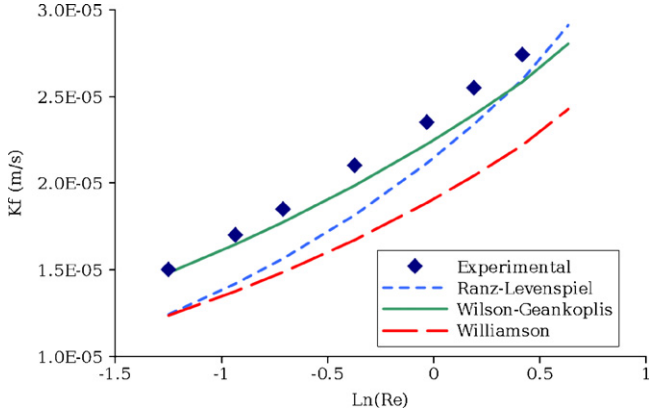

Fig. 3. Comparison of the external mass-transfer coefficients evaluated from experimental measurement or estimated through correlations.

Table 2
Correlations proposed for the determination of the external transfer coefficient K_f.

Authors	Correlation	Domain of validity
Williamson et al. [30]	$Sh = 2.4\epsilon\, Re^{0.34}\, Sc^{0.42}$	$0.08 < Re < 125$ $150 < Sc < 1300$
Wilson and Geankoplis [31]	$Sh = 1.09\epsilon^{-2/3}\, Re^{1/3}\, Sc^{1/3}$	$0.0016 < \varepsilon Re < 55$ $950 < Sc < 70,000$ $0.35 < \epsilon < 0.75$
Yoshida et al. [32]	$Sh = 0.91\, Sc^{1/3} A[\epsilon\psi Re]^{0.49}$ $A = [6(1-\epsilon)]^{0.51}$	$Re < 55$ $\psi = 1$ for spheres $\psi = 0.91$ for cylinders
Kunii and Levenspiel [33]	$Sh = 2 + 1.8\, Re^{1/2} Sc^{1/3}$	
Ohashi [34]	$Sh = 2 + 1.58\, Re^{0.4}\, Sc^{1/3}$	$0.001 < Re < 5.8$

for $0.25 < Re < 2$ with a bed porosity of $\epsilon = 0.524$. The value of the Reynolds number exponent falls within the [0.33–0.5] range corresponding to the correlations reported in the literature (Table 2).

3.4. Validity of the model

The experimental and modelled breakthrough curves at different flow rates are plotted in Fig. 4 and a very good agreement between the experimental and simulated curves is achieved. As the flow rate increases the breakthrough curves become steeper as generally reported in the case of phenol solutions passed through active carbon beds [7] or other adsorbents such as resins [12]. This observation has also been reported for other aromatic pollutants [23]. Indeed with a Biot number (Eq. (2)) close to 10 for a flow rate of $0.245 \times 10^{-6}\ m^3/s$, the curves fall within the 2nd category of classification defined by Hand et al. [20]. Breakthrough curves in the categories 1 (steeper) and 2 show sigmoidal profile and are most commonly found in organic pollutants adsorption onto activated carbon [27].

$$Bi = \frac{K_f \cdot d_P \cdot C^0}{2 \cdot D_e \cdot \rho_p \cdot q_e} \tag{2}$$

In order to validate the model and the values of the parameters, it is necessary to compare the value of the critical time for the experimental and calculated breakthrough curves. Fig. 5 shows that for an inlet concentration $C^0 = 5\ kg/m^3$ and a critical concentration fixed at $C_{crit} = 0.3 \times 10^{-3}\ kg/m^3$ the difference between the experimental and calculated critical time is low enough to be acceptable at low flow rate. However for flow rates larger than $0.245 \times 10^{-6}\ m^3/s$ and at the beginning of the breakthrough curves the calculated outlet concentration value tends to be overestimated as compared with the experimental one which leads to a shift between the curves (cf. insert).

3.5. Sensitivity study

The parameters for which the sensitivity of the modelling was investigated are either a characteristic of the adsorbant d_P the mean carbon grain diameter, or of the substrate or of its interaction with the adsorbant such as:

- D_e, the effective diffusivity
- K_f, the mass-transfer coefficient
- k_L the adsorption constant of the Langmuir isotherm equation
- q_{max} the maximum uptake of substrate adsorbed on AC

Indeed the mean carbon grain diameter can be measured with the required precision (it is an outer model parameter in the sense of Sperlich et al. [27]) but since the model does not take into account the size dispersion of the adsorbant grain, it is worth to evaluate the model sensitivity to this parameter in order to estimate the trends for the effect on the critical time of grain size variation (such as those caused by attrition). The other parameters (inner model parameters in the sense of Sperlich et al.) are either measured [5] (k_L, q_{max}, K_f) or estimated via correlations (D_e, K_f) and it is important to estimate how error in their determination could affect the

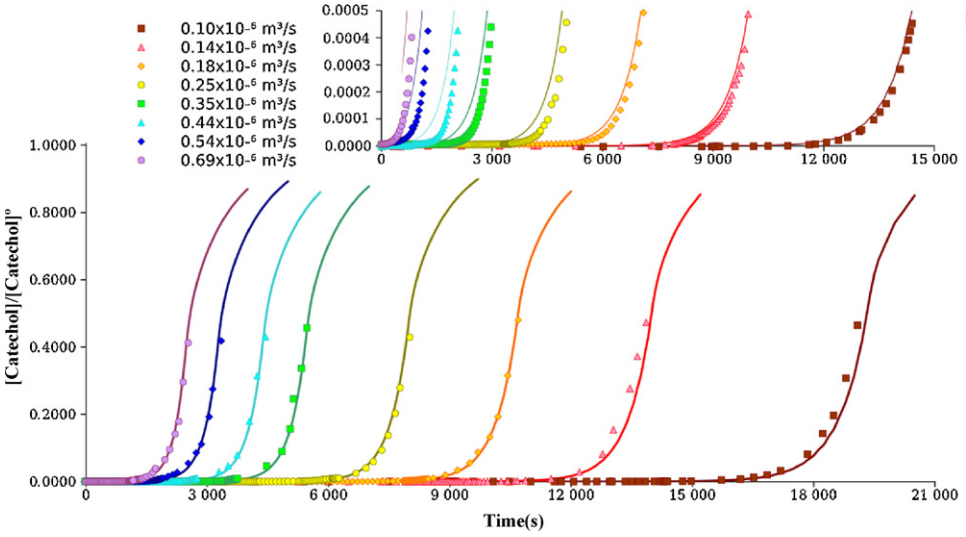

Fig. 4. Experimental and modelled breakthrough curves ($C^0 = 5\ kg/m^3$).

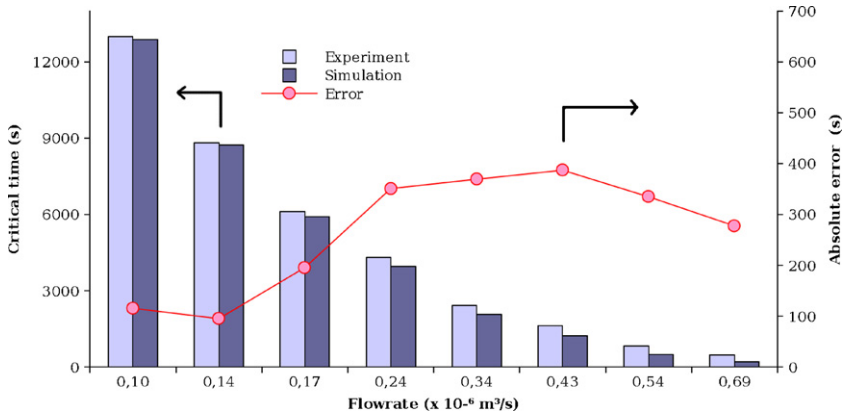

Fig. 5. Comparison of the critical time measured experimentally or derived from simulation as a function of the flow rate.

Table 3
Parameters and operating conditions used for the modelling of the reference breakthrough curve.

Operating conditions	
Active charcoal mass	$m = 31$ g
Initial concentration	$C^0 = 5\,\text{kg/m}^3$
Solution flow	$Q_l = 2.45 \times 10^{-7}\,\text{m}^3/\text{s}$
Adsorbant characteristics	
Bed specific mass	$\rho_t = 460\,\text{kg/m}^3$
Bed porosity	$\epsilon_B = 0.524$
Particle specific mass	$\rho_p = 966\,\text{kg/m}^3$
Particle diameter	$d_P = 800\,\mu\text{m}$
Substrate parameters	
Effective diffusivity	$D_e = 1.4 \times 10^{-11}\,\text{m}^2/\text{s}$
Mass-transfer coefficient in the liquid phase	$K_f = 2.1 \times 10^{-5}\,\text{m/s}$
Adsorption capacity	$q_{\max} = 0.32\,\text{g/g}_{\text{carbon}}$
Langmuir adsorption constant	$k_L = 75\,\text{g/L}$
Critical concentration	$C_{\text{crit}} = 0.3 \times 10^{-3}\,\text{kg/m}^3$
Reduced critical concentration	$C^*_{\text{crit}} = C_{\text{crit}}/C^0 = 6 \times 10^{-5}$

accuracy of the critical time computed using the model. Table 3 shows the values of the parameters used in the modelling of a typical breakthrough curve.

Figs. 6–10 show the effects of the variation of these parameters upon the shape and position of the breakthrough curves and more particularly upon the estimated critical time.

From these figures, it appears that K_f and d_P have the biggest effect upon the critical time and this makes sense since at the beginning of the adsorption external mass transfer is the dominant kinetic resistance.

This emphasizes the importance of a correct value for the mass transfer coefficient in order to obtain a useful predictive value of the critical time by modelling. Indeed the use of under- or overestimated value for K_f within the same order of magnitude (which is not unusual in chemical engineering) leads to dramatic changes in the predicted critical time.

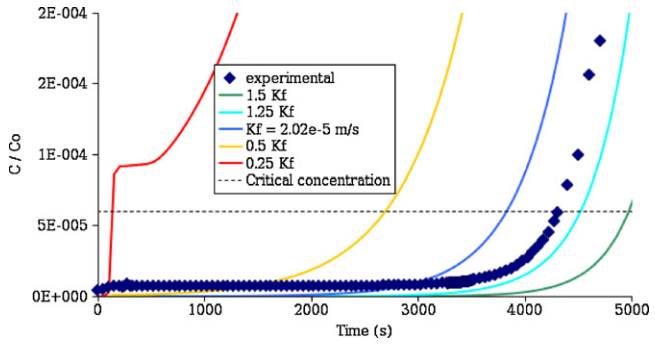

Fig. 6. Sensitivity of the breakthrough curve with the mass-transfer coefficient (K_f).

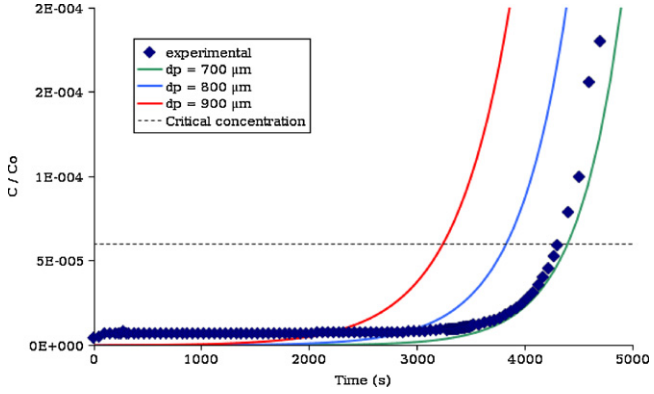

Fig. 7. Sensitivity of the breakthrough curve with the active charcoal particle diameter (d_P).

The importance of the mean particle size value is also great as shown in Fig. 7 all the more that the effect of the adsorbant grain size distribution has not been considered.

The effect of the diffusivity D_e upon the critical time is much less dramatic (Fig. 8), indeed a 50% increase of the value of this parameter leads only to a 6% increase of the critical time. Higher values of D_e are associated with stiffer curves. However when the outlet concentration is risen, the shift between the curves plotted with different values of D_e increases. This means that the intra-granular diffusion becomes the rate-controlling mechanism, but this only occurs for values of the outlet concentration well above the critical concentration. This small sensitivity of the diffusion coefficient is related

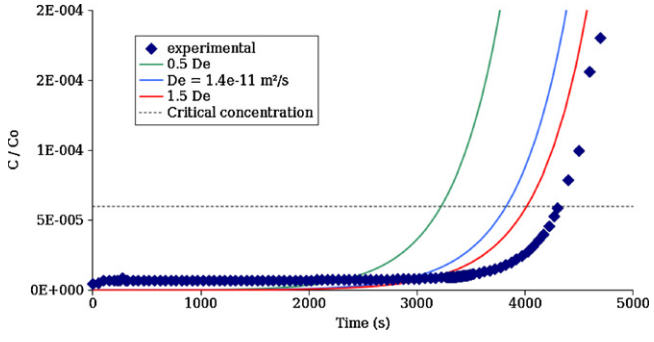

Fig. 8. Sensitivity of the breakthrough curve with the effective diffusion coefficient (D_e).

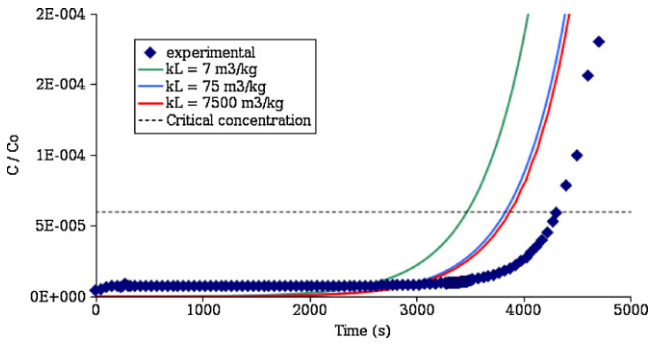

Fig. 9. Sensitivity of the breakthrough curve with the Langmuir adsorption constant (k_L).

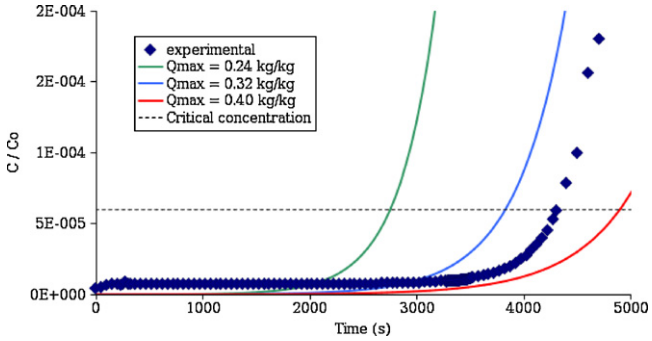

Fig. 10. Sensitivity of the breakthrough curve with the active charcoal adsorption capacity (q_{max}).

to the class of breakthrough curve as defined by Hand et al. [20]. Indeed curves of the 3rd category ($Bi > 30$) have been reported to be highly sensitive to the diffusion coefficient as in the case of pentachlorophenol adsorption by activated carbon [22] which suggests that for larger molecules diffusion within the pores may become the limiting mechanism in the adsorption process.

Fig. 9 shows that the Langmuir constant k_L of the isotherm has a very limited effect upon the critical time. Indeed its value has to be changed by at least an order of magnitude to produce a significant variation of t_C. This means that the use of a more complex isotherm equation could not improve the accuracy of the modelling.

And last, the variation of the adsorption capacity q_{max} leads to an expected shift of the breakthrough curve (Fig. 10) since a lower adsorption capacity necessarily leads to a shorter retention of the pollutant on the column. This decrease of the critical time with the adsorption capacity comes with a stiffening of the curve. The variation of the adsorption capacity for a fixed amount of adsorbent is equivalent to a variation of the amount of adsorbent (or bed height) with a fixed capacity, i.e. results in a capacity of adsorption of the bed. The result observed is consistent with the literature where a reduction of the bed capacity comes together with a stiffening of the breakthrough curves [7].

4. Conclusions

The main results pointed out by the present study are:

- The existence of an optimal flow of polluted effluent through the adsorbing bed to achieve the removal of the pollutant from the solution with a high efficiency. In the case of 5 kg/m^3 solutions of catechol the optimal flow rate vs. adsorbant mass was found to be about 0.02 m^3 h^{-1} kg^{-1}.
- The HSDM model allows for the prediction of experimental breakthrough curves, as well as the critical time. The best agreement are achieved at low flow rates.
- The parameter that most affect the value of the critical time are the mass-transfer coefficient K_f and the adsorbant mean particle diameter d_P. The adsorption isotherm pattern is not a governing parameter for critical time estimation.
- In order to obtain a good estimation of the critical time through modelling it is necessary to use an accurate value of the mass-transfer coefficient K_f, either from a correlation established in similar condition or better from experimental measurement using the SBA method.
- The model validated and its parameters evaluated with lab-scale experiments can been used to estimate the scale-up for the design of units able to handle larger flow rates. However the larger pressure drops generated then should be taken into account.
- The behavior of other pollutants (such as the phenolic compounds encountered in olive oil mill waste waters [5]) could also be predicted provided their effective diffusivity can be estimated.

Acknowledgements

This work was made with the financial support of the CNRS. María de Lourdes Delgado-Núñez acknowledges the grant of leave given by the Universidad Autónoma Metropolitana and the support of the CONACYT-Mexico.

Appendix A. Derivation of the equations

Hydrodynamic dispersion is accounted for by the mixing cell in series model [37]. The different equations representing the physical phenomena involved in each cell i (total number $Ncell$) are:

Mass balance equation in the liquid phase

$$Q_l \cdot (C_{b,i-1} - C_{b,i}) = \frac{m}{N_{cell}} \cdot \frac{dq_{av.,i}}{dt} + \frac{\epsilon_B \cdot V_{bed}}{N_{cell}} \cdot \frac{dC_{b,i}}{dt} \quad (A.1)$$

$$q_{av.,i}(t) = \frac{3}{(d_p/2)^3} \cdot \int_0^{d_p/2} q_i(r,t) \cdot r^2 \cdot dr \quad (A.2)$$

Intraparticular diffusion

$$\frac{\partial q_i(r,t)}{\partial t} = \frac{D_e}{r^2} \cdot \left\{ \frac{\partial (r^2 \cdot (\partial q_i(r,t)/\partial r))}{\partial r} \right\} \quad (A.3)$$

Liquid–solid equilibrium at the interface

$$\frac{q_{s,i}(t)}{q_{max}} = \frac{k_L \cdot C_{s,i}(t)}{1 + k_L \cdot C_{s,i}(t)} \quad (A.4)$$

Initial conditions

$$q_i(r,0) = C_{b,i}(0) = C_{s,i}(0) = 0 \quad (A.5)$$

Boundary conditions (symmetry at the center of the grain, flux through its surface)

$$\left(\frac{\partial q_i(r,t)}{\partial r} \right)_{r=0} = 0 \quad (A.6)$$

$$\rho_p \cdot D_e \cdot \left(\frac{\partial q_i(r,t)}{\partial r} \right)_{r=d_p/2} = K_f \cdot (C_{b,i} - C_{s,i}) \quad (A.7)$$

In order to solve this equation system and determine $C_b(t)$, dimensionless variables are used. This equation system cannot be solved analytically and the numerical integration method is carried

out using the *orthogonal collocation* method developed by Villadsen and Stewart [38] over the particle radius, leading to a system with five equations and five unknowns for each stirred reactor of the model. The numerical resolution of this system is carried out with a variable step integration method (derived from the ones described in "Numerical Recipes in FORTRAN" [39]) which gives the value of each unknown in each stirred reactor as a function of time. From where the average value of the adsorbed pollutant in each cell and the effluent concentration at the column outlet is immediately derived.

References

[1] G. Achilli, G.P. Cellerino, P.H. Gamache, G.M. d'Eril, Identification and determination of phenolic constituents in natural beverages and plant extracts by means of a coulometric electrode array system, J. Chromatogr. 632 (1993) 111–117.

[2] G.M. Hunt, E.A. Baker, Phenolic constituents of tomato cuticle, Phytochemistry 19 (1980) 1415–1419.

[3] V. Félis, P. Fouilloux, C.D. Bellefon, D. Schweich, Three-step catalytic detoxication of waste water containing chloroaromatics: experimental results and modelisation issues, Ind. Eng. Chem. Res. 38 (1999) 4213–4219.

[4] D. Richard, M.de L. Delgado-Núñez, C. de Bellefon, D., Schweich, Ch. 55: Depollution of waters contaminated by phenols and chlorophenols using catalytic hydrogenation, in: Environmental Chemistry—Green Chemistry and Pollutants in Ecosystems, Springer, 2004, pp. 601–613.

[5] D. Richard, M. de Lourdes Delgado-Núñez, D. Schweich, Adsorption of complex phenolic compounds on active charcoal: Adsorption capacity and isotherms, Chem. Eng. J. 148 (2009) 1–7.

[6] A. Dabrowski, P. Podkoscielny, Z. Hubicki, M. Barczak, Adsorption of phenolic compounds by activated carbon—a critical review, Chemosphere 58 (2005) 1049–1070.

[7] A.C. Lua, Q. Jia, Adsorption of phenol by oil-palm-shell activated carbons in a fixed bed, Chem. Eng. J. 150 (2009) 455–461.

[8] P. Cañizares, M. Carmona, O. Baraza, A. Delgado, M.A. Rodrigo, Adsorption equilibrium of phenol onto chemically modified activated carbon F400, J. Hazard. Mater. B131 (2006) 243–248.

[9] G. Vázquez, R. Alonso, S. Freire, J. González-Álvarez, G. Antorrena, Uptake of phenol from aqueous solutions by adsorption in a *Pinus pinaster* bark packed bed, J. Hazard. Mater. 133 (2006) 61–67.

[10] Z. Aksu, F. Gönen, Biosorption of phenol by immobilized activated sludge in a continuous packed bed: prediction of breakthrough curves, Process Biochemistry 39 (2004) 599–613.

[11] M. Otero, M. Zabkova, A.E. Rodrigues, Comparative study of the adsorption of phenol and salicylic acid from aqueous solution onto nonionic polymeric resins, Sep. Purif. Technol. 45 (2005) 86–95.

[12] B. Pan, F. Meng, B.P.X.Q. Chen, X. Li, W. Zhang, X. Zhang, J. Chen, Q. Zhang, Y. Sun, Application of an effective method in predicting breakthrough curves of fixed-bed adsorption onto resin adsorbent, J. Hazard. Mater. B 124 (2005) 74–80.

[13] A. Adak, A. Pal, Removal of phenol from aquatic environment by SDS-modified alumina: Batch and fixed bed studies, Sep. Purif. Technol. 50 (2006) 256–262.

[14] W.J. Weber, E.H. Smith, Simulation and design model for adsorption processes, Environ. Sci. Technol. 21 (1987) 1040–1050.

[15] W. Whitman, The two film theory of gas absorption, Chem. Metal. Eng. 29 (1923) 146–148.

[16] T.W. Weber, R.K. Chakravorty, Pore and solid diffusion models for fixed-bed adsorbers, AIChE J. 20 (1974) 228–237.

[17] U.K. Traegner, M.T. Suidan, Evaluation of surface and film diffusion coefficients for carbon adsorption, Water Res. 23 (1989) 267–273.

[18] V.K.C. Lee, J.F. Porter, G. McKay, Fixed bed modelling for acid dye adsorption onto activated carbon, J. Chem. Technol. Biotechnol. 78 (2003) 1281–1289.

[19] A.A. Susu, Mathematical modelling of fixed bed adsorption of aromatics and sulphur compounds in kerosene deodorisation, Chem. Eng. Process. 39 (2000) 485–497.

[20] D. Hand, J. Crittenden, W.E. Thacker, Simplified models for design of fixed-bed adsorption systems, J. Environ. Eng. 110 (1984) 440–456.

[21] D. Chatzopoulos, A. Varma, Aqueous-phase adsorption and desorption of toluene in activated carbon fixed deds: experiments and model, Chem. Eng. Sci. 50 (1995) 127–141.

[22] A.J. Slaney, R. Bhamidimarri, Adsorption of pentachlorophenol (PCP) by activated carbon in fixed beds. application of homogeneous surface diffusion model, Water Sci. Technol. 38 (1998) 227–235.

[23] J.-M. Chern, Y.-W. Chien, Adsorption isotherms of benzoic acid onto activated carbon and breakthrough curves in fixed-bed columns, Ind. Eng. Chem. Res. 40 (2001) 3775–3780.

[24] J.L. Sotelo, M.A. Uguina, J.A. Delgado, L.I. Celemin, Adsorption of methyl ethyl ketone and trichloroethene from aqueous solutions onto activated carbon fixed-bed adsorbers, Sep. Purif. Technol. 37 (2004) 149–160.

[25] V.K.C. Lee, G. McKay, Comparison of solutions for the homogeneous surface diffusion model applied to adsorption systems, Chem. Eng. J. 98 (2004) 255–264.

[26] A.L. Ahmad, S. Chong, M.F. Bhatia, Prediction of breakthrough curves for adsorption of complex organic solutes present in palm oil mill effluent (POME) on granular activated carbon, Ind. Eng. Chem. Res. 45 (2006) 6793–6802.

[27] A. Sperlich, S. Schimmelpfennig, B. Baumgarten, A. Genz, G. Amy, E. Worch, M. Jekel, Predicting anion breakthrough in granular ferric hydroxide (GFH) adsorption filters, Water Res. 42 (2008) 2073–2082.

[28] A. Sperlich, A. Werner, A. Genz, G. Amy, E. Worch, M. Jekel, Breakthrough behavior of granular ferric hydroxide (GFH) fixed-bed adsorption filters: modeling and experimental approaches, Water Res. 39 (2005) 1190–1198.

[29] T. Furusawa, J. Smith, Fluid-particle and intraparticle mass transport rates in slurries, Ind. Eng. Chem. Fundamen. 12 (1973) 197–203.

[30] J.E. Williamson, K.E. Bazaire, C.J. Geankoplis, Liquid-phase mass transfer at low Reynolds numbers, Ind. Eng. Chem. Fundam. 2 (1963) 126–129.

[31] E.J. Wilson, C.J. Geankoplis, Liquide mass transfer at very low Reynolds numbers in packed beds, Ind. Eng. Chem. Fundam. 5 (1966) 9–14.

[32] F. Yoshida, D. Ramaswami, A. Hougen, Temperature and partial pressures at the surfaces of catalyst particles, AIChE J. 8 (1962) 5–11.

[33] D. Kunii, O. Levenspiel, Fluidization Engineering, Wiley, New York, 1969.

[34] H. Ohashi, Liquide mass transfer in packed beds, J. Chem. Eng. Jpn. 14 (1981) 433–438.

[35] K.T. Liu, W.J. Weber Jr., Characterization of mass transfer parameters for adsorber modeling and desing, J. Water Pollut. Control Fed. 53 (1981) 1541–1550.

[36] W.J. Weber, K.T. Liu Jr., Determination of mass transport parameters for fixed-bed adsorbers, Chem. Eng. Commun. 6 (1980) 49–60.

[37] C.Y. Wen, L.T. Fan, Models for Flow Systems and Chemical Reactors, Marcel Dekker, 1975.

[38] J.V. Villadsen, W.E. Stewart, Solution of boundary-value problems by orthogonal collocation, Chem. Eng. Sci. 22 (1967) 1483–1501.

[39] W.H. Press, W.T. Vetterling, S.A. Teukolski, B.P. Flannery, Numerical recipes in Fortran: The art of scientific computing, Cambridge University Press, New York, 1992.